Bull. Chem. Soc. Ethiop. **2024**, 38(2), 511-526.
DOI: https://dx.doi.org/10.4314/bcse.v38i2.18

ISSN 1011-3924
Printed in Ethiopia
Online ISSN 1726-801X

GEOMETRY OPTIMIZATION AND ENERGY PARAMETER CALCULATIONS USING DENSITY-FUNCTIONAL THEORY METHOD AND MOLECULAR DOCKING OF ANTICONVULSANT THERAPEUTIC METAL COMPLEXES OF GABAPENTIN

Amnah Mohammed Alsuhaibani[1], Moamen S. Refat[2*], Abdel Majid A. Adam[2], Mohamed I. Kobeasy[2] Mohamed Y. El-Sayed[3] and Kareem A. Asla[4]

[1]Department of Physical Sport Science, College of Education, Princess Nourah bint Abdulrahman University, P.O. Box 84428, Riyadh 11671, Saudi Arabia
[2]Department of Chemistry, College of Science, Taif University, P.O. Box 11099, Taif 21944, Saudi Arabia
[3]Chemistry Department, College of Science, Jouf University, Sakaka 2014, Saudi Arabia
[4]Department of Chemistry, Faculty of Science, Zagazig University, Zagazig, 44519, Egypt

(Received August 31, 2023; Revised November 24, 2023; Accepted November 25, 2023)

ABSTRACT. This work aims to give computational studies of Mn(II), Co(II), Ni(II) and Cu(II) complexes of gabapentin (Gpn), formulized as $[M(Gpn)(H_2O)_3(Cl)].nH_2O$ complexes (where n = 2-6), using DFT method. They were previously synthesized and characterized. DFT calculations are in good agreement with practical studies. Bond lengths of metal complexes reduced or increased rather than that of ligand due to complexation. Bond angles of complexes predict the octahedral environment around the central metal ions predicting sp^3d^2 or d^2sp^3hybridization. The calculated energy parameters are negative indicating stability of metal complexes. The small energy band gap of compounds predicts the higher biological activity and high tendency of electron transfer. The comparable frequencies of theoretical and experimental IR may be attributed to different phases of measurement. The induced fit docking SP G-score of the molecular interactions of drug (Gpn) and its metal(II) complexes show that all investigated compounds have a good interaction towards sertonine receptor 5-HT2C and D2 dopamine receptor proteins. Co(II)-Gpn interacts with active site residues of sertonine receptor 5-HT2C with an excellent dock score of -7.370 kcal/mol and RMSD = 1.581 Å. On the other hand, Ni(II)-Gpn has the best dock score of -6.638 kcal/mol and RMSD = 1.995 Å with D2 dopamine receptor.

KEY WORDS: Gabapentin, Transition metals, DFT-method, molecular docking

INTRODUCTION

Anaesthesiologists claim that the usage of preoperative opioids as relievers has declined. Gabapentin (Gpn) has had a significant impact in this progress [1]. The anticonvulsant gabapentin, which belongs to the second generation, is efficient in the treatment of persistent neuropathic pain as well as it is advantageous in severe perioperative circumstances [2, 3]. Gpn, lessens confusion, afterwards dizziness, vomiting, and chronic post-surgical pain [3, 4]. Gpn, also known as Neurontin. It belongs to the class of gamma-aminobutyric acid, $C_9H_{17}NO_2$. It is taken in conjunction with other medications to treat various psychiatric conditions, anxiousness, and dyskinesia as well as to prevent epilepsy [3, 5, 6]. It is a synthetic amino acid containing both acidic (COOH) and basic (NH_2) groups [7, 8]. Gpn has two pKa values; 3.7 and 10.0 for (COOH) and (NH_2), respectively and is zwitterionic at pH = 0 [9]. diverse metal complexes of gabapentin with La^{3+}, Ce^{3+}, Nd^{3+}, Y^{3+}, and Mn^{2+} have been synthesized characterized [10, 11]. Biological potent Zn(II) and Cu(II) complexes of gabapentin were also reported [12]. The cobalt and nickel metal complexes with Gpn were synthesized and investigated to be more potent than Gpn [13]. Gp-Au(III) complexes have been prepared and investigated to have medicinal potential [14, 15].

*Corresponding author. E-mail: moamen@tu.edu.sa ; msrefat@yahoo.com

As an effective cancer-preventing, antibacterial, and antimycotic pharmaceuticals, Gpn-AgNPs were studied to be compatible with upcoming nanodrugs that may hold great promise for drug delivery [16]. Gpn metal complexes were synthesized by solid state reaction of zinc and Cu salts with solid Gpn [17]. The Cu^{2+}, Ni^{2+}, Cd^{2+}, Co^{2+} and Zn^{2+} metal complexes of Gpn have been prepared in solution with (1:2) molar ratio (M:L) [18]. The correlation between the ionisation potential, electron affinity, electronegativity, electrophilicity index, hardness, and chemical potential was revealed using the HOMO and LUMO analyses for Gpn and its compounds using DFT method [19-21]. The molecular docking of gabapentin-cobalt complex has been investigated and gives better activity rather than Gpn [13]. The Mn(II), Co(II), Ni(II) and Cu(II) metal complexes of gabapentin (Gpn), formulized as $[Mn(Gpn)(H_2O)_3(Cl)].4H_2O$, $[Co(Gpn)(H_2O)_3(Cl)].6H_2O$, $[Cu(Gpn)(H_2O)_3(Cl)].2H_2O$, and $[Ni(Gpn)(H_2O)_3(Cl)].3H_2O$ complexes, have been already synthesized and full characterized in our previous work [22]. In this paper, the quantum chemistry calculations for Gpn and its metal complexes already synthesized were checked using the material studio software as integral applications for published work. The structures have been optimized and give good agreement with experimental suggestions. Furthermore, molecular properties based on the structure were determined for bond lengths, bond angles, atomic charges, total energy, electronic properties, and frontier molecular orbitals energy in a gaseous environment. Theoretical vibrational frequencies of Gpn have been recorded at range 4000-400 cm^{-1}. The energy values of HOMO and LUMO predicts the charge transfer inside the molecule. The charge density distribution and chemical reactivity of Gpn are given by MEP. Dipole-moment, total, binding energies, and others have been computed. Furthermore, molecular docking of (Gpn) and its metal(II) complexes towards sertonine receptor 5-HT2C and D2 dopamine receptor proteins have been studied.

EXPERIMENTAL

Synthesis of (Gpn) metal complexes

Gabapentin metal complexes (Figure 1) were prepared and fully characterized as discussed in our previous work [22]. The FTIR spectral data of $[Mn(Gpn)(H_2O)_3(Cl)].4H_2O$, $[Co(Gpn)(H_2O)_3(Cl)].6H_2O$, $[Cu(Gpn)(H_2O)_3(Cl)].2H_2O$, and $[Ni(Gpn)(H_2O)_3(Cl)].3H_2O$ complexes were recorded.

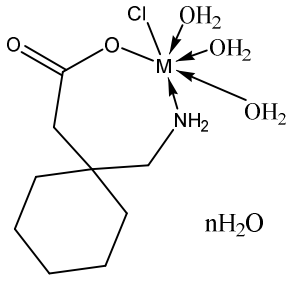

Figure 1. The structure of synthesized Mn(II), Co(II), Ni(II) and Cu(II)-Gpn complexes, where, n = 2 for Cu(II), 3 for Ni(II), 4 for Mn(II) and 6 Co(II).

Geometry optimization

Utilizing the $DMOL^3$ program from the Materials Studio package [23], computational studies were carried out [24-26]. Double numerical basis sets and polarization functional (DNP) were

used in the computations of DFT semi-core pseudopods (dspp) [27]. The generalized gradient approximation (GGA), the best correlation functional, serves as the foundation for the RPBE functional [28, 29].

Molecular docking

I. Preparation of ligand. The default protocol of the Ligprep program in the Schrodinger's suite [30] has been utilized for molecular docking of the drug (Gpn) and its Co^{II}, Mn^{II}, Ni^{II}, and Cu^{II} metal complexes. Using the induced fit receptor docking with SP protocol glide redocking, all compounds were docked to the target protein. Docking employs the SP protocol as well as post-docking reduction. For the best-docked ligands, the SP G-score was employed as a ranking parameter.

II. Protein specification. Protein Data Banking was used to download the 3D complex structures of the 5-HT_{2C} sertonine receptor (PDB ID: 6BQH) and the D2 dopamine receptor (PDB ID: 6CM4) [31, 32]. The D2 Dopamine receptor is better matching the interaction with gabapentin because it is considered one of the best receptors used in the treatment of many diseases and medical disorders such as Parkinson's disease, hyperprolactinemia, nausea and vomiting. Moreover, dopamine is used in targeted drugs to treat substance abuse such as amphetamines, cocaine, and opioids [32]. Additionally, drugs that target several serotonin receptors are useful in treating obesity, substance abuse and schizophrenia. Serotonin is also a potential therapeutic target for depression, schizophrenia, drug addiction, and other disorders [31]. The protein preparation wizard program from the Schrödinger suite [33], the protein structures have been constructed by removing water molecules (> 5A radius) as well as other tiny molecules from the structural section. The PDB structures were modified by adding hydrogens and forming disulphide linkages. The optimized potential for liquid simulations (OPLS-2005) force field has been exposed to confined imperf minimization using default settings. Induced fit receptor docking had been applied to the resultant structures. The resultant data was evaluated using the XP G-score and RMSD, where RMSD stands for root mean square deviation, expressed in units of Å, from the original ligand (positive control) which in our study were Ritanserin, and Risperidone that originally binds to protein; sertonine receptor 5-HT2C (PDB ID: 6BQH) and D2 dopamine receptor (PDB ID: 6CM4) [31, 32]. The induced fit docking can be accomplished using precision SP, which involves utilizing the sample ring confirmation of ligands with a binding strength of 2.5 kcal/mol, as well as the receptor inner box of 10 Å and auto outer box. The parameters for induced fit docking are binding site A:2001 and A:1201 for Dopamine and Sertonine receptors, respectively, with trim side chains of receptor van der waals scaling 0.70 kcal/mol, ligand van der waals scaling 0.50 kcal/mol, and employing the forcefield OPLS_2005. Additionally, the refinement of the ligand distance cutoff is limited to within 5.0 Å. Finally, induced redocking into the receptor within 30 kcal/mol of the 20 best ligand structures.

RESULTS AND DISCUSSION

DFT studies

Using the density functional theory (DFT) method, the molecular modelling was created, and several energetic parameters were estimated, including bond length, bond angle, chemical reactivity, MEP, total energy, dipole moment, and binding energy for drug ligand and its metal complexes. The optimized molecular structures of the gabapentin ligand and its metal complexes are displayed in structures 1-6, along with an atom numbering scheme. Data listed in Tables 2S-6S of the optimized bond lengths and bond angles for gabapentin and its metal complexes, and from these data the following remarks have been concluded: (i) The bond lengths of gabapentin

(Gpn) moiety is slightly altered; the most substantial change is triggered in C(7)-N(8), N(8)-H(25), N(8)-H(26), C(10)-O(12), O(9)-C(10) and O(9)-H(27) bond lengths which, as a result of bonding, are either decreased or increased upon complexation [34]. (ii) The bond angles in $[Ni(L)(H_2O)_3Cl]$ and $[Mn(L)(H_2O)_3Cl]$ complexes are close to octahedral geometry, which predicts sp^3d^2 or d^2sp^3 hybridization. Furthermore, $[Co(L)(H_2O)_3Cl]$ and $[Cu(L)(H_2O)_3Cl]$ complexes show distorted Oh geometry [35]. (iii) A strong M-O bond forms, shortening the C(10)-O(9) bond distance for gabapentin complexes while lengthening C(10)-O(12) bond distance of the carbonyl group, making the C-O bond weaker [36]. Because the M-N bond forms and weakens the C-N bond, the C(7)-N(8) bond distance lengthens in all gabapentin complexes [37]. (iv) As a result of the stronger bonds between Mn-N and Cu-N, their bond distances in $[Mn(L)(H_2O)_3Cl]$ and $[Cu(L)(H_2O)_3Cl]$ complexes are shorter than those between Ni-N and Co-N in those complexes. In gabapentin complexes, the M-O bond distances are comparable, indicating that the bond strength will also be comparable.

The chemical reactivity and site selectivity of the molecular frameworks are explained by the density function theory (DFT) approach. For the gabapentin ligand and its metal complexes Structures 7-18, the energies of the frontier molecular orbitals (EHOMO, ELUMO), energy band gap that explains the inevitable charge exchange cooperation within the molecule, electronegativity (χ), chemical potential (μ), global hardness (η), global softness (S), and global electrophilicity index (ω) [38-40] have been computed using Equations 1-5 and are shown in Table 1.

$$\chi\ (\text{electronegativity}) = -\frac{1}{2}\left(E_{LUMO} + E_{HOMO}\right) \quad (1)$$

$$\mu\ (\text{potential}) = -\chi = \frac{1}{2}\left(E_{LUMO} + E_{HOMO}\right) \quad (2)$$

$$\eta\ (\text{hardness}) = \frac{1}{2}\left(E_{LUMO} - E_{HOMO}\right) \quad (3)$$

$$S\ (\text{softness}) = \frac{1}{2}\eta \quad (4)$$

$$\omega\ (\text{electrophilicity}) = \frac{\mu^2}{2\eta} \quad (5)$$

The term "softness", σ, is used to refer to the inverse of the global hardness, as seen in the following: $\sigma = 1/\ \eta$.

According to data reported in Table 1, as the molecular weight of a compound increases, the gas phase energy declines. The calculated energy parameters are negative indicating that the prepared compounds are stable [41]. In contrast to LUMO energy, which is closely associated to nucleophilic attack reactivity, HOMO energy is closely related to electrophilic attack reactivity. The coordination sites for an electrophilic attack can be predicted using the frontier orbital theory. The narrow energy gap for the gabapentin ligand facilitates the flow of charge and consequently this can be used in biological as well as solar cells applications. It is easier to characterize the kinetic stability and chemical reactivity of molecules because of the small energy band gap, which can also provide a considerable stability index. Moreover, the small energy band gap of gabapentin confers it a strong propensity to coordinate metal ions especially that the HOMO level is mostly localized on the oxygen and nitrogen atoms of (C-O) and (N-C) bonds [39]. The higher HOMO energy of molecule enhances its ability to donate electrons to the lower LUMO energy [42]. Global hardness (η) and global softness (S) are important characteristics to gauge the stability and reactivity of molecules. A soft molecule has a lower value for its energy gap compared to a hard one. The metal ion functions as a Lewis acid during complex formation, whereas the ligand functions as a Lewis base. Because metal ions are soft acids, soft base ligands are best for forming complexes with them. This leads to the conclusion that a correct value (S) gabapentin ligand has a good propensity to efficiently chelate metal ions [40]. The computed chemical potential (μ) supports this as well. One of the most crucial quantum chemical descriptors for defining the reactivity and sites that contribute to the toxicity of different contaminants is the electrophilicity index [41]. Electrophilicity also accurately measures the biological activity of

drug receptor contact. This new reactivity index gauges the energy stabilization that occurs when a system picks up an extra electrical charge from its surroundings. The higher total energy (ΔE_{tot}) of nickel(II) and cobalt(II) complexes are -8.88×10^5 and -9.04×10^5 kcal/mol, respectively corresponding to higher electrophilicity index (ω/ev) reflecting the high potency of those compounds. Nickel(II) and cobalt(II) complexes show good interaction with protein according to the later molecular docking studies. For the gabapentin ligand and its metal complexes, the energy components (total energy, binding energy, and dipole moment) were determined using the DFT approach outlined in Tables 2. According to the computed binding energy, the metal chelate has a larger binding energy than the ligand. This suggests that the produced metal complexes are more stable than free ligand.

Table 1. Calculated E_{HOMO}, E_{LUMO}, energy band gap ($E_H - E_L$), chemical potential (μ), electronegativity (χ), global hardness (η), global softness (S), global electrophilicity index (ω) and softness (σ) for gabapentin ligand and its metal complexes.

Compound	E_H/Ev	E_L/Ev	$_H$-E_L/ ev	χ/ev	μ/ev	η/ev	S/ev^{-1}	ω/ev	σ/ev^{-1}
Gabapentin ligand	-5.143	-0.845	-4.298	2.994	-2.994	1.0745	0.5372	4.1712	0.930
Gabapentin (Enol)	-4.874	-0.325	-4.549	2.5995	-2.599	1.1372	0.5686	2.9709	0.8793
[Co(L)$(H_2O)_3$Cl]	-3.783	-3.014	-0.769	3.3985	-3.3985	0.1922	0.0961	30.038	5.2015
[Ni(L)$(H_2O)_3$Cl]	-4.528	-2.822	-1.706	3.675	-3.675	0.4265	0.2132	15.833	2.344
[Mn(L)$(H_2O)_3$Cl]	-2.281	-0.852	-1.429	1.5665	-1.566	0.3572	0.1786	3.4344	2.799
[Cu(L)$(H_2O)_3$Cl]	-4.454	-0.301	-4.153	2.3775	-2.377	1.0382	0.5191	2.7221	0.963

Table 2. Some energetic properties of gabapentin ligand and its metal complexes calculated by DMOL^3 method using DFT- method.

Compound	Total energy (kcal/mol)	Binding energy (kcal/mol)	Dipole moment (D)
Gabapentin	-3.51E+05	-2928.171	3.4303
Gabapentin (enol)	-3.51E+05	-2935.100	13.3110
[Co(L)$(H_2O)_3$Cl]	-8.88E+05	-3748.008	12.3257
[Ni(L)$(H_2O)_3$Cl]	-9.04E+05	-3747.850	6.9831
[Mn(L)$(H_2O)_3$Cl]	-8.59E+05	-3679.268	5.8734
[Cu(L)$(H_2O)_3$Cl]	-9.23E+05	-3677.101	16.6612

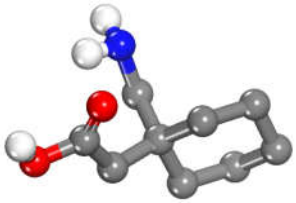

Structure 1: The optimized geometry of gabapentin (keto form)

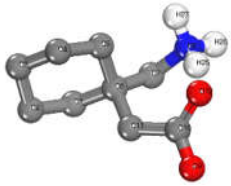

Structure 2: The optimized geometry of gabapentin (enol form)

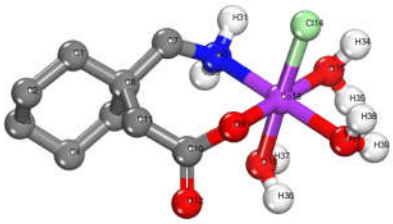

Structure 3 : The optimized geometry of $[Co(L)(H_2O)_3Cl]$ complex

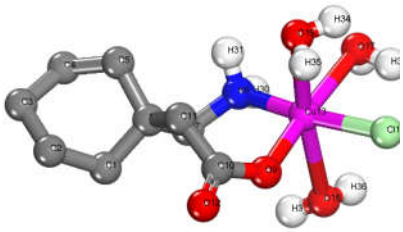

Structure 4: The optimized geometry of $[Cu(L)(H_2O)_3Cl]$ complex

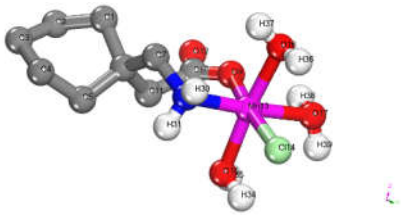

Structure 5 : The optimized geometry of $[Mn(L)(H_2O)_3Cl]$ complex

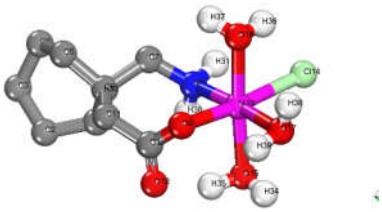

Structure 6 : The optimized geometry of $[Ni(L)(H_2O)_3Cl]$ complex

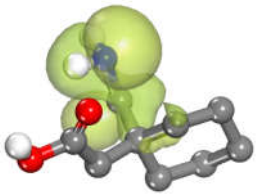

Structure 7: The optimized geometry of HOMO of gabapentin

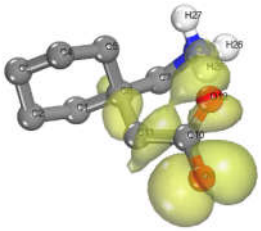

Structure 8 : The optimized geometry of HOMO of gabapentin (enol form)

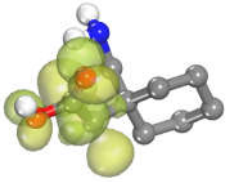

Structure 9: The optimized geometry of LUMO of gabapentin (keto)

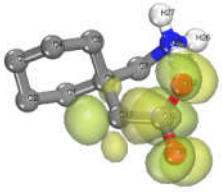

Structure 10: The optimized geometry of LUMO of gabapentin (enol)

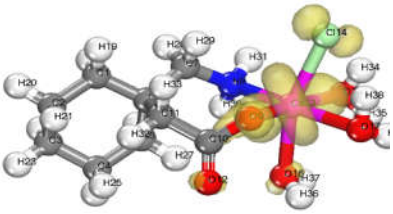

Structure 11: The optimized geometry of HOMO of $[Co(L)(H_2O)_3Cl]$ Complex

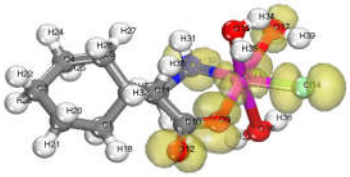

Structure 12: The optimized geometry of HOMO of $[Cu(L)(H_2O)_3Cl]$ complex

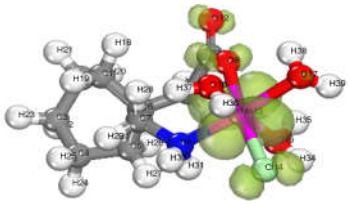

Structure 13: The optimized geometry of HOMO of $[Mn(L)(H_2O)_3Cl]$ complex

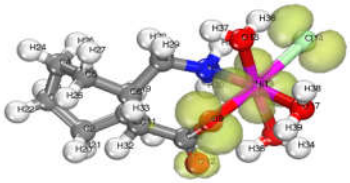

Structure 14: The optimized geometry of HOMO of $[Ni(L)(H_2O)_3Cl]$ complex

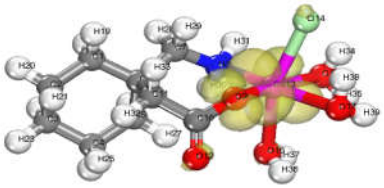

Structure 15: The optimized geometry of LUMO of $[Co(L)(H_2O)_3Cl]$ Complex

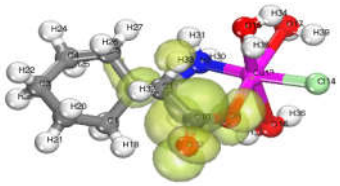

Structure 16: The optimized geometry of LUMO of $[Cu(L)(H_2O)_3Cl]$ Complex

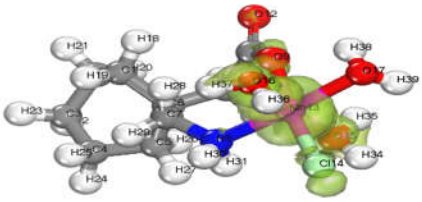

Structure 17: The optimized geometry of LUMO of $[Mn(L)(H_2O)_3Cl]$ complex

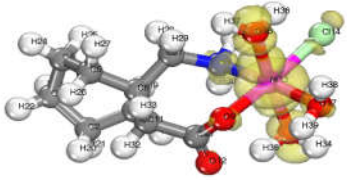

Structure 18: The optimized geometry of LUMO of $[Ni(L)(H_2O)_3Cl]$ complex

Molecular electrostatic potential (MEP)

The MEP is a sketch of the electrostatic potential V(r) at a given point r (x, y, z) onto the surface of constant electron density. Additionally, it is extremely helpful in the study of molecular

structure along with its physicochemical properties as well as hydrogen bonding interactions [43-47]. Figs. 2, 3 show the 3D plots of keto and enol forms of gabapentin. The red color indicates the high electron density which is the potential site for electrophilic attack. However, the blue color indicates the electron deficient region that is more likely for the nucleophilic attack. Potential increases in the color's red, green, and blue, with blue displaying the most attraction and red the strongest repulsion. The oxygen and nitrogen atoms have regions of negative potential (nitrogen and oxygen atoms have high negative values; N(8)= -0.926, O(9) = -0.533, O(12) = -0.523) however, the regions above the hydrogen and carbon atoms (the high positive values belong to C(26) = +0.352, C(10) = +0.579) are those with a positive potential.

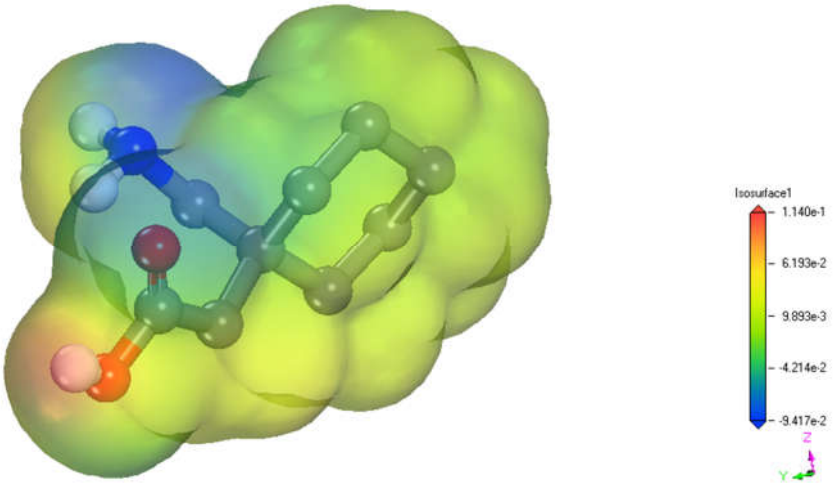

Figure 2. Molecular electrostatic potential map for gabapentin (keto form).

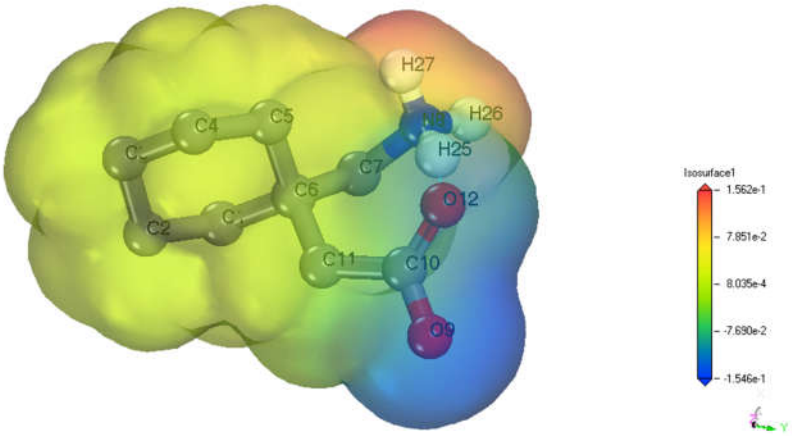

Figure 3. Molecular electrostatic potential map for gabapentin (enol form).

Theoretical IR spectra for gabapentin ligand

An insight to fig. 4, there is a small deviation between the computed and the experimental infrared frequencies. This may be attributed to the frequency calculations of the molecule that have been computed in vacuum while experimental IR spectra were measured for solid sample. Due to the low symmetry of ligands, the vibrational modes are extremely complex. In particular, the in-plane, out-of-plane, and torsion modes lead to the difficulty to assign most of vibrational modes [48]. Nevertheless, the IR spectrum contains a few potent frequencies that are relevant for characterization.

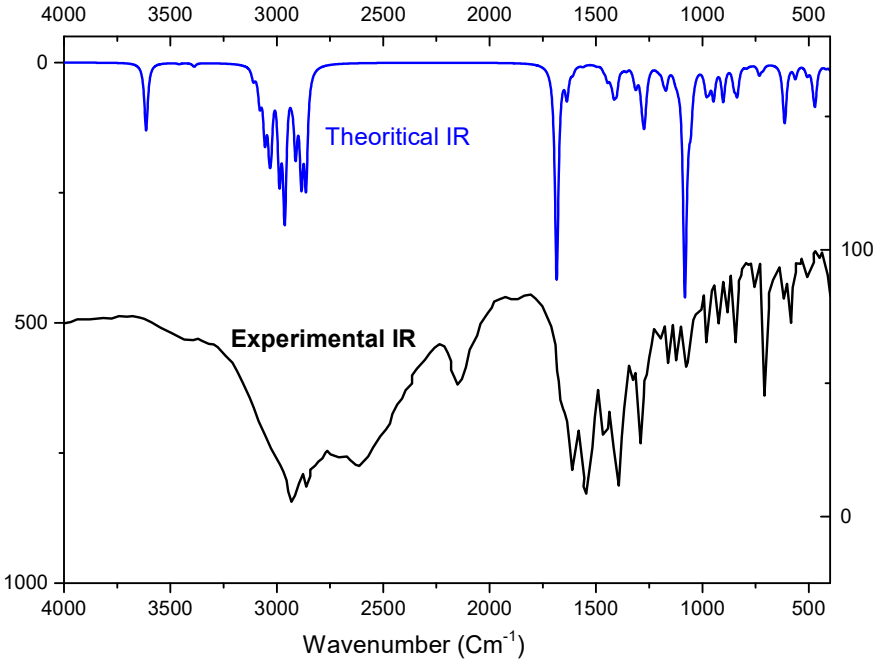

Figure 4. Experimental IR versus theoretical IR spectra of gabapentin.

Molecular docking

Figures 5 and 6, show the 3D molecular interactions of drug (Gpn) in its two forms; keto and zwitterion forms as well as its metal(II) complexes. The Dotted lines in the below figures (each yellow and purple) refer to H-bonding and halogen bonds or salt bridge, respectively between protein and drug (Gpn) entity. The 2D representations of the interactions between the drug in both structures and the serotonin receptor 5-HT2C and D2 dopamine receptor proteins are shown in Figures 7 and 8. Figure 7a shows the interaction between Gpn in its zwitterion form and D2 dopamine, revealing that the residues TYR408←H_2O→(C-O^-), HIE393→H_2O→(C-O^-), TYR408→(C=O), and (NH_3^+)→ASP114 had established hydrogen bonds. Additionally, (NH_3^+)----ASP134 showed Salt bridge interactions. Figure 7b shows the interaction between Gpn in keto form and serotonin, revealing that the residues SER193←H_2O→(C=O), HIE393→H_2O→(C=O), (NH_2)→ASP114, and (NH_2)→TYR418 had established hydrogen bond. Figure 8a shows the interaction between Gpn in its zwitterion form and serotonin, revealing that the residues

LEU209←H_2O→(C=O), LEU20→(C-O^-), and (NH_3^+)→ASP134 had established hydrogen bonds. Additionally, (NH_3^+)----ASP134 showed Salt bridge interactions. Figure 8b shows the interaction between Gpn in keto form and serotonin, revealing that the residues LEU209←H_2O→(OH) had established hydrogen bond. The results with docking XP G-score Tables 3 and 4 exhibits that all investigated have an interaction towards serotonin receptor 5-HT2C and D2 dopamine receptor proteins. The highest G-score (-7.370 kcal/mol and RMSD = 1.581 Å) belongs to Co(II)-Gpn complex indicating the good interaction with the active site of serotonin receptor. However, Ni(II)-Gpn has the best dock score of -6.638 kcal/mol and RMSD= 1.995 Å with D2 dopamine receptor. According to the data tabulated in Table 3 and 4, the following remarks have been concluded. As a glance of one can conclude the following remarks: (i) Gpn has the low SP G-score values (-3.982 kcal/mol) towards D2 dopamine receptor and relatively greater value of binding potential (-4.649 kcal/mol) towards sertonine receptor 5-HT2C. This suggests the stronger interaction of GPn-serotonin rather than GPn-dopamine. However, in case of zwitterions of Gpn with serotonin and dopamine the values of binding energies are relative (-5.528 and -5.588 kcal/mol) for sertonine receptor 5-HT2C and D2 dopamine, respectively. (ii) The only interaction of Cu(II)-Gpn with D2 dopamine receptor is Solvent exposure (Figure 6f). (iii) Most interactions of investigated compounds with both receptors were hydrogen bonds. Moreover, Gpn as Zwitterions structure exhibits H-bonds as well as one salt bridge of NH_3^+ with the amino acid ASP134 (Figures 5b and 6b). (iv) Co(II)-Gpn have three interactions with sertonine receptor 5-HT2C *via* hydrogen bond (LEU209→(C=O), H_2O→ASP134 and (NH_2)→ASP134) with distances 1.70, 1.56 and 2.02 Å, respectively (Figure 5d). While, the interaction of Ni(II)-Gpn with D2 dopamine receptor through hydrogen bond ASP114←H_2O→(C=O) and H_2O→THR412 with distance (1.55, 1.90) and 1.67 Å, respectively (Figure 6e).

Table 3. Molecular interactions with serotonin receptor 5-HT2C (6BQH).

compound	Interactions	Type	distance (Å)	SP G-score	RMSD (Å)
Gpn	←H_2O→(OH)		1.75, 1.69		
Gpn (Zwitterions structure)	LEU209←H2O→(C=O) LEU20→(C-O-) (NH3+)→ASP134 (NH3+)----ASP134	H-bond H-bond H-bond Salt bridge	1.75, 1.70 1.93 1.67 2.62	-5.528	1.389
Mn(II)-Gpn	LEU209→(C=O) H2O→ASP134 (NH2)→ASP134	H-bond H-bond H-bond	2.54 1.61 2.36	-4.954	1.893
Co(II)-Gpn	LEU209→(C=O) H2O→ASP134 (NH2)→ASP134	H-bond H-bond H-bond	1.70 1.56 2.02	-7.370	1.581
Ni(II)-Gpn	LEU209→(C=O) (NH2)→ASP134	H-bond H-bond	2.53 2.24	-6.083	1.683
Cu(II)-Gpn	LEU209→(C=O) H2O→ASP134 (NH2)→ASP134	H-bond H-bond H-bond	1.82 1.48 1.90	-6.204	1.460

SP G-score: kcal mol^{-1}.

Table 4. Molecular interactions with D2 dopamine receptor (6CM4).

compound	Interactions	Type	distance (Å)	SP G-score	RMSD (Å)
Gpn	SER193←H2O→(C=O) HIE393→H2O→(C=O) (NH2)→ASP114 (NH2)→TYR418	H-bond H-bond H-bond H-bond	1.75, 2.11 1.67, 2.11 1.86 1.95	-3.982	1.916
Gpn (Zwitterions structure)	TYR408←H2O→(C-O-) HIE393→H2O→(C-O-) TYR408→(C=O) (NH3+)→ASP114 (NH3+)----ASP134	H-bond H-bond H-bond H-bond Salt bridge	1.77, 1.97 1.70, 1.97 1.71 1.86 2.72	-5.588	1.128
Mn(II)-Gpn	ASP114←H2O→(C=O)	H-bond	1.76, 2.10	-5.681	0.938
Co(II)-Gpn	ASP114←H2O→(C=O) NH2→ASP114	H-bond H-bond	1.50, 1.14 2.47	-4.086	1.376
Ni(II)-Gpn	ASP114←H2O→(C=O) H2O→THR412	H-bond H-bond	1.55, 1.90 1.67	-6.638	1.995
Cu(II)-Gpn	Solvent exposure	---	---	-5.514	0.905

SP G-score: kcal mol^{-1}.

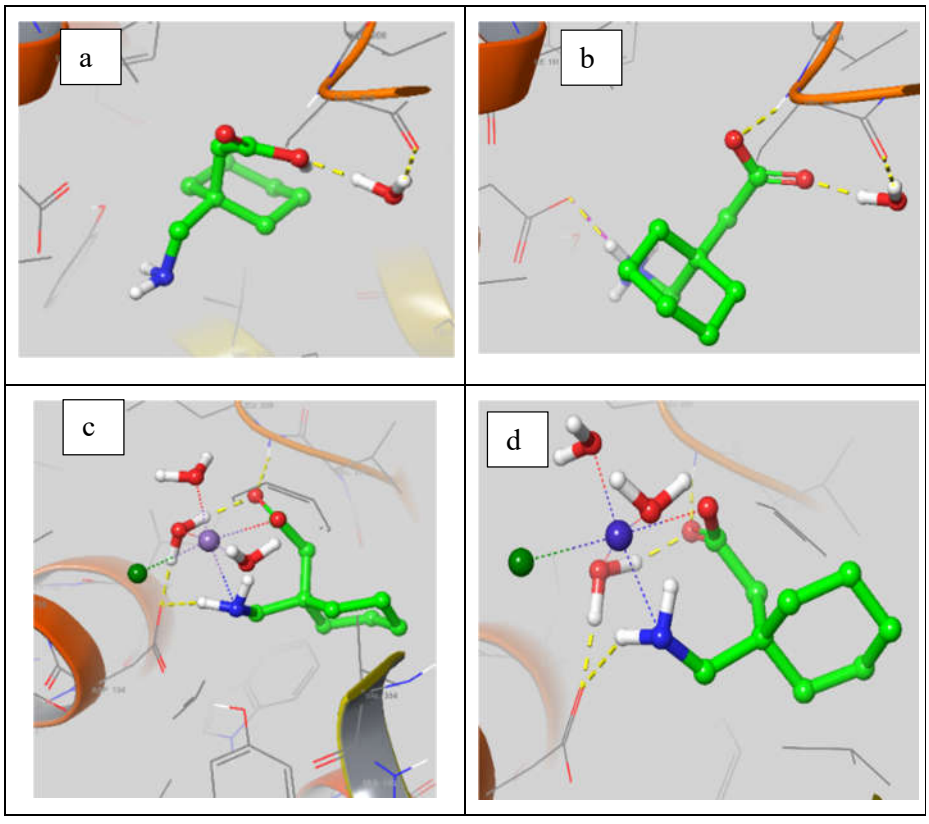

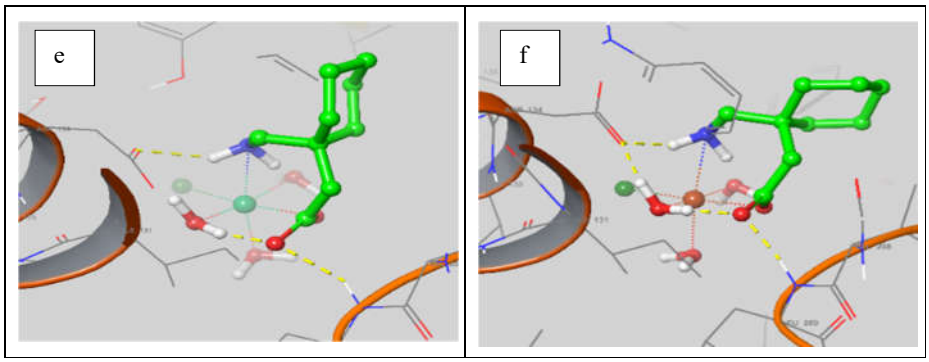

Figure 5. 3D molecular interaction of (a) gabapentin, (b) gabapentin (Zwitterions structure), (c) Mn(II)-gabapentin, (d) Co(II)-gabapentin, (e) Ni(II)-gabapentin and (f) Cu(II)-gabapentin with sertonine receptor 5-HT2C (6BQH).

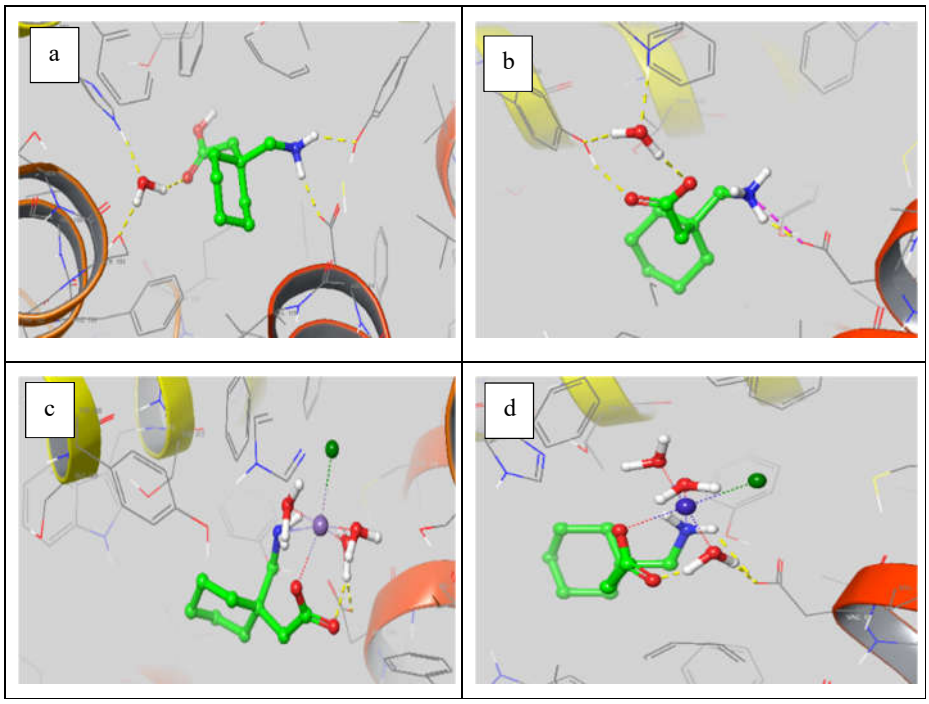

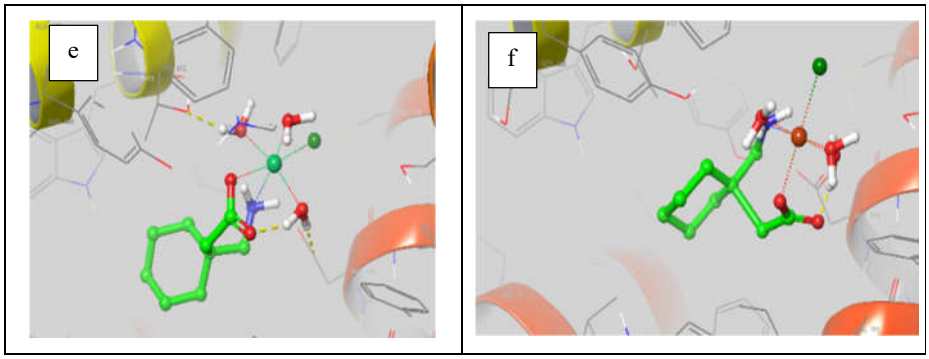

Figure 6. 3D molecular interaction of (a) gabapentin, (b) gabapentin (Zwitterions structure), (c) Mn(II)-gabapentin, (d) Co(II)-gabapentin, (e) Ni(II)-gabapentin and (f) Cu(II)-gabapentin with D2 dopamine receptor (6CM4).

CONCLUSION

In this paper, as a complementary studying to what has been done, four Mn(II), Co(II), Ni(II) and Cu(II) metal complexes of gabapentin (Gpn) as well as (Gpn) have been studied using DFT method. The previous study have suggested that the metal complexes have the general formulae of $[M(Gpn)(H_2O)_3(Cl)].nH_2O$ (where n = 2-6). Those compounds were synthesized and fully characterized with known physicochemical as well as spectral studies. Geometry optimization and the energy calculations show that (i) the computed bond lengths of all metal complexes are reduced or increased rather than that of (Gpn) ligand may be attributed to complexation. (ii) The calculated bond angles of all metal complexes predict the octahedral environment (sp3d2 or d2sp3 hybridization) around the central metal ions. (iii) The negative values of the calculated energy parameters indicate stability of all metal complexes. (iv) The smaller band gap of all metal complexes rather than (Gpn) predicts the facility of electron transfer from HOMO to LUMO. (v) The comparable frequencies of theoretical and experimental IR may be attributed to different phases of measurement. The docking XP G-score of the molecular interactions of drug (Gpn) and its metal(II) complexes show that all investigated compounds have a good interaction towards sertonine receptor 5-HT2C and D2 dopamine receptor proteins. The docking XP G-score shows (i) an excellent dock score of -7.370 kcal/mol and RMSD = 1.581 Å for Co(II)-Gpn compound suggesting that there is good interaction with active site residues of sertonine receptor 5-HT2C. (ii) On the other hand, Ni(II)-Gpn has the best dock score of -6.638 kcal/mol and RMSD = 1.995 Å˚with D2 dopamine receptor.

ACKNOWLEDGEMENT

The researchers would like to acknowledge Deanship of Scientific Research, Taif University for funding this work.

REFERENCES

1. Chen, O.; Cadwell, J.B.; Konstantina, M.; Hagen, J.; Afonson, A.M. Perioperative gabapentin usage in pediatric patients: A scoping review. *Pediatr. Anesth*. **2023**, 33, 598-608.
2. Taylor CP. Emerging perspectives on the mechanism of action of gabapentin. *Neurology* **1994**, 44, S10-S16.

3. Eisenberg, E.; River, Y.; Shifrinand, A.; Krivoy, N. Antiepileptic drugs in the treatment of neuropathic pain. *Drugs* **2007**, 67, 1265-1289.
4. Ameringen, M.V.; Rynn, M.A.; Murphy, T.K.; Mandel, F. Influence of gender on the clinical presentation of generalized anxiety disorder, and response to treatment with Pregabalin. *Eur. Psych.* **2008**, 23, S221-S222.
5. Jensen, A.A.; Mosbacher, J.; Elg, S. The anticonvulsant gabapentin (neurontin) does not act through γ-aminobutyric acid-B receptors. *Mol. Pharmacol.* **2002**, 61, 1377.
6. Sills, G.J. The mechanisms of action of gabapentin and pregabalin. *Curr. Opin. Pharmacol.* **2006**, 6, 108-113.
7. Satzinger, G. Antiepileptics from gamma-aminobutyric acid. *Forsch.* **1994**, 44, 261-266.
8. Schwarz, J.B.; Gibbons, S.E.; Graham, S.R.; Colbry, N.L.; Guzzo, P.R.; Le, V.D.; Vartanian M.G.; Kinsora, J.J.; Lotarski S.M.; Zheng, L.; Dickerson, M.R.; Su, T.; Weber, M.L.; El-Kattan, A.; Thorpe A.J.; Donevan, S.D.; Taylor, C.P.; Wustrow, D.J. Novel cyclopropyl β-amino acid analogues of pregabalin and gabapentin that target the α2-δ protein. *J. Med. Chem.* **2005**, 48, 3026-3035.
9. Alrawashdeh, L.; Kulaib, B.F.; Assaf, K.I.; El-Barghouthi, M.I.; Bodoor, K.; Abuhasan, O.M.; Abdoh, A.A. Cucurbit[7]uril complexes with gabapentin: Effect on lactamization. *J. Mol. Liq.* **2003**, 380, 121716.
10. Nadgi, A.; Mhlong, N.; Esoliman, M. Metal complexes in cancer therapy update from drug design perspective. *Drug Des. Devel. Ther.* **2017**, 11, 599-618.
11. Quaresma, S.; Andre, V.; Antunes, A.M.M.; Cunha-Silva, L.; Duarte, M.T. Gabapentin coordination networks: Mechanochemical synthesis and behavior under shelf conditions. *Cryst. Growth Des*. **2013**, 13, 5007-5017.
12. Braga, D.; Grepioni, F.; Maini, L.; Brescello, R; Cortarca, L. Simple and quantitative mechanochemical preparation of the first zinc and copper complexes of the neuroleptic drug gabapentin. *Cryst. Eng. Comm.* **2008**, 10, 469-471.
13. Amshumali, M.K.; Abhilash, N.; Patil, M. Unprecedented example of metal complexes with 1-aminomethyl-1-cyclohexane acetic acid. *Int. J. Chem. Sci.* **2018**, 16, 289.
14. Shaikjee, A.; Levendis, D.C.; Marques, H.M.; Mampa, R. A gold(III) complex and a tetrachloroaurate salt of the neuroepileptic drug gabapentin. *Inorg. Chem. Commun.* **2011**, 14, 534-538.
15. Levendis, D.C.; Shaikjee, A.; Marques, H.M.; Mampa, R. A gold(III) complex of the neuroepileptic drug gabapentin, *Acta Crystallogr.* **2011**, A67, C585.
16. Yaseen, B.; Gangwar, C.; Nayak, R.; Kumar, S.; Sarkar, Joy.; Banerjee, M.; Naik, R.M. Gabapentin loaded silver nanoparticles (GBP-AgNPs) for its promising biomedical application as a nanodrug: Anticancer and Antimicrobial activities. *Inorg. Chem. Commun.* **2023**, 149, 110380.
17. Braga, D.; Grepioni, F.; Maini, L.; Brescellob, R.; Cotarcab, L. Simple and quantitative mechanochemical preparation of the first zinc and copper complexes of the neuroleptic drug gabapentin. *Cryst. Eng. Comm.* **2008**, 10, 469-471.
18. Abd-Alrassol, K.S.; Qasim, Q.A.; Shari, F.H.; AL-Salman, H.N.K.; Hussein, H.H. The spectrophotometric determination of antiepileptic drug in standard and pharmaceutical formulations by diazotization coupling reaction and some metal complexes. *Syst. Rev. Pharm.* **2020**, 11, 247-260.
19. Khezri, B.; Maskanati, M.; Zohrevand, B.; Liyaghati-Delshad, M.; Soltanali, F. Theoretical investigation of adsorption of the gabapentin drug on the heteroborospherene. *Struc. Chem.* **2022**, 33, 315-322.
20. Yang, L.; Li, D.; Guo, B.; Wei, D. Theoretical study on the inclusion interaction of β-cyclodextrin with gabapentin and its stability. *J. Struc. Chem.* **2019**, 60, 564-574.

21. Ganeshvar, P.S.; Kanagaraj, M.; Gunasekaran, S.; Gnanasambandan T. Experimental and theoretical investigation of gabapentin by density functional theory. *Int. J. Sci. Eng.* **2016**, 7, 8-15.
22. Refat, M.S.; Gaber, A.; Althobaiti, Y.S.; Alyami, H.; Alsanie, W.F.; Shakya, S.; Adam, A.M.A.; Kobeasy M.I.; Asla, K.A. Spectroscopic and molecular docking studies of Cu(II), Ni(II), Co(II), and Mn(II) complexes with anticonvulsant therapeutic agent gabapentin. *Molecules* **2022**, 27, 4311.
23. Kessi, A.; Delley, B. Density functional crystal vs. cluster models as applied to zeolites. *Int. J. Quantum Chem*. **1998**, 68, 135-144.
24. Delley, B. A scattering theoretic approach to scalar relativistic corrections on bonding. *Int. J. Quantum Chem*. **1998**, 69, 423-433.
25. Delley, B. From molecules to solids with the DMol3 approach. *J. Chem. Phys.* **2000**, 113, 7756-7764.
26. El-Rayyes, A.; Mogharbel, R.T.; Abdel-Rhman, M.H.; Ismail, M.A.; Abdel-Latif, E. Molecular geometry and biological activity of 2-(4-substituted-phenylimino)thiazolidin-4-one compounds. *Bull. Chem. Soc. Ethiop*. **2023**, 37, 1275-1286.
27. Al-Resayes, S.I.; Jarad, A.J.; Al-Zinkee, J.M.M.; Al-Noor, T.H.; El-ajaily, M.M.; Abdalla, M.; Min, K.; Azam, M.; Mohapatra, R.K. Synthesis, characterization, antimicrobial studies, and molecular docking studies of transition metal complexes formed from a benzothiazole-based azo ligand. *Bull. Chem. Soc. Ethiop*. **2023**, 37, 931-944.
28. Sreedevi, R.; Sinthiya, A.S.I.J.; Beaula, T.J.; Balu, T.; Murugakoothan, P. Growth, characterization and chemical computations of guanidinium trichloroacetate (GTCA) single crystal – DFT approach. *Bull. Chem. Soc. Ethiop*. **2023**, 37, 1033-1045.
29. Hammer, B.; Hansen, L.B.; Nrskov, J.K. Improved adsorption energetics within density-functional theory using revised Perdew-Burke-Ernzerhof functionals. *Phys. Rev. B* **1999**, 59, 7413-7421.
30. Ahmad, S.; Bhanu, P.; Kumar, J.; Pathak, R.K.; Mallick, D.; Uttarkar, A.; Niranjan, V.; Mishra, V. Molecular dynamics simulation and docking studies reveal NF-κB as a promising therapeutic drug target for COVID-19. *Bioinformation* **2021**, 18, 170-179.
31. Peng, Y.; Peng, Y.; McCorvy, J.D.; Harpsøe, K.; Lansu, K.; Yuan, S.; Popov, P.; Qu, L.; Pu, M.; Che, T.; Nikolajsen, L.F.; Huang, X.; Wu, Y.; Shen, L.; Bjørn-Yoshimoto, W.E.; Ding, K.; Wacker, D.; Han, G.W.; Cheng, J.; Katritch, V.; Jensen, A.A.; Hanson, M.A.; Zhao, S.; Gloriam, D.E.; Roth, B.L.; Stevens, R.C.; Liu, Z.J. 5-HT2C receptor structures reveal the structural basis of GPCR polypharmacology. *Cell* **2018**, 172, 719-730.
32. S. Wang, T. Che, A. Levit, B.K. Shoichet, D. Wacker, B.L. Roth, Structure of the D2 dopamine receptor bound to the atypical antipsychotic drug risperidone. *Nature* **2018**, 555, 269-273.
33. Schrödinger Release 2023-4: Canvas, Schrödinger, LLC: New York; **2023**.
34. West, D.X.; Swearingen, J.K.; Valdes-Martınez, J.; Hernandez-Ortega, S.; El-Sawaf, A.K.; van Meurs, F.; Castineiras, A.; Garcia, I.; Bermejo, E. Spectral and structural studies of iron(III), cobalt(II,III) and nickel(II) complexes of 2-pyridineformamide N(4)-methylthiosemicarbazone. *Polyhedron* **1999**, 18, 2919-2929.
35. Despaigne, A.A.R.; Da Silva, J.G.; Do Carmo, A.C.M.; Piro, O.E.; Castellano, E.E.; Beraldo, H. Copper(II) and zinc(II) complexes with 2-benzoylpyridine-methyl hydrazone. *J. Mol. Struct.* **2009**, 920, 97-102.
36. Hocking R.K.; Hambley T.W. Structural measure of metal-ligand covalency from the bonding in carboxylate ligands. *Inorg. Chem.* **2003**, 42, 2833-2835.
37. Pearson, R.G. Absolute electronegativity and hardness: applications to organic chemistry. *J. Org. Chem.* **1989**, 54, 1423-1430.

38. El-Sherif, A.A.; Fetoh, A.; Abdulhamed, Y.Kh.; Abu El-Reash, G.M. Synthesis, structural characterization, DFT studies and biological activity of Cu(II) and Ni(II) complexes of novel hydrazone. *Inorg. Chim. Acta* **2018**, 480, 1-15.
39. El-Reash, G.A.; El-Gammal, O.; Ahmed, F. Molecular structure and biological studies on Cr(III), Mn(II) and Fe(III) complexes of heterocyclic carbohydrazone ligand. *Spectrochim. Acta Mol. Biomol. Spectrosc.* **2014**, 121, 259-267.
40. Yousef, T.A.; Abu El-Reash, G.M.; El Morshedy, R.M. Quantum chemical calculations, experimental investigations and DNA studies on (E)-2-((3-hydroxynaphthalen-2-yl) methylene)-N-(pyridin-2-yl)hydrazinecarbothioamide and its Mn(II), Ni(II), Cu(II), Zn(II) and Cd(II) complexes. *Polyhedron* **2012**, 45, 71-85.
41. Parthasarathi, R.; Padmanabhan, J.; Subramanian, V.; Sarkar, U.; Maiti, B.; Chattaraj, P. Toxicity analysis of benzidine through chemical reactivity and selectivity profiles: A DFT approach. *Intenet. Electron. J. Mol. Design.* **2003**, 2, 798-813.
42. Kandil, S.S.; El-Hefnawy, G.B.; Baker, E.A. Thermal and spectral studies of 5-(phenylazo)-2-thiohydantoin and 5-(2-hydroxyphenylazo)-2-thiohydantoin complexes of cobalt(II), nickel(II) and copper(II). *Thermochim. Acta* **2004**, 414, 105.
43. Sagdinc, S.; Koksoy, B.; Kandemirli, F.; Bayari, S.H. Theoretical and spectroscopic studies of 5-fluoro-isatin-3-(*N*-benzylthiosemicarbazone) and its zinc(II) complex. *J. Mol. Struct*. **2009**, 63, 917.
44. Luque, F.J.; López, J.M.; Orozco, M. Perspective on "Electrostatic interactions of a solute with a continuum. A direct utilization of ab initio molecular potentials for the prevision of solvent effects". *Theor. Chem. Acc.* **2000**, 103, 345.
45. Okulik, N.; Jubert, A.H. Theoretical analysis of the reactive sites of non–steroidal anti–inflammatory drugs. *Internet. Electron. J. Mol. Des.* **2005**, 4, 17-30.
46. Scrocco, E.; Tomasi, J. The electrostatic molecular potential as a tool for the interpretation of molecular properties. New concepts II, Springer: Berlin; **1973**; p. 170.
47. Politzer, P.; Laurence, P.R.; Jayasuriya, K. Molecular electrostatic potentials: An effective tool for the elucidation of biochemical phenomena. *Environ. Health Perspect*. **1985**, 61, 191-202.
48. Lu, Y.; Wang, Y.; Jiang, Z.; Men, Y. Molecular weight dependency of surface free energy of native and stabilized crystallites in isotactic polypropylene. *ACS Macro. Lett.* **2014**, 3, 1101-1105.